Multidim Syst Sign Process (2014) 25:795–828
DOI 10.1007/s11045-013-0232-9

General formulation of shift and delta operator based 2-D VLSI filter structures without global broadcast and incorporation of the symmetry

I.-Hung Khoo · Hari C. Reddy · Lan-Da Van · Chin-Teng Lin

Received: 18 October 2011 / Revised: 1 March 2013 / Accepted: 6 March 2013 /
Published online: 21 March 2013

Abstract Having local data communication (without global broadcast of signals) among the elements is important in very large scale integration (VLSI) designs. Recently, 2-D systolic digital filter architectures were presented which eliminated the global broadcast of the input and output signals. In this paper a generalized formulation is presented that allows the derivation of various new 2-D VLSI filter structures, without global broadcast, using different 1-D filter sub-blocks and different interconnecting frameworks. The 1-D sub-blocks in z-domain are represented by general digital two-pair networks which consist of direct-form or lattice-type FIR filters in one of the frequency variables. Then, by applying the sub-blocks in various frameworks, 2-D structures realizing different transfer functions are easily obtained. As delta discrete-time operator based 1-D and 2-D digital filters (in γ-domain) were shown to offer better numerical accuracy and lower coefficient sensitivity in narrow-band filter designs when compared to the traditional shift-operator formulation we have covered both the conventional z-domain filters as well as delta discrete-time operator based filters. Structures realizing general 2-D IIR (both z- and γ-domains) and FIR transfer functions (z-domain only) are presented. As symmetry in the frequency response reduces the complexity of the design, IIR transfer functions with separable denominators, and transfer functions with quadrantal magnitude symmetry are also presented. The separable denominator

This paper is dedicated to Professor Eli Jury on the occasion of his 90th birthday this year (2013). Professor Jury has been a pioneer in modern digital control and multidimensional systems. It was Professor Jury who has encouraged the second author (Hari C. Reddy) to use delta discrete time operator in the study of 1-D and M-D systems and filters. This was followed by the doctoral dissertation of the first author (I-Hung Khoo) on the topic at the University of California, Irvine in 2002. This is a simple token of appreciation to Professor Jury for his mentoring, friendship and guidance.

I.-H. Khoo (✉) · H. C. Reddy
Department of Electrical Engineering, California State University Long Beach, Long Beach, CA, USA
e-mail: ikhoo@csulb.edu

H. C. Reddy
College of Computer Science, National Chiao-Tung University, HsinChu City, Taiwan

L.-D. Van · C.-T. Lin
Department of Computer Science, National Chiao-Tung University, HsinChu City, Taiwan

frameworks are needed for quadrantal symmetry structures to guarantee BIBO stability and thus presented for both the operators. Some limitations of having exact symmetry with separable 1-D denominator factors are also discussed.

Keywords 2-D filters · Delta operator · Symmetry · VLSI

1 Introduction

Two-dimensional (2-D) digital filters find applications in many digital signal processing areas such as image processing, beamforming (Joshi et al. 2012), and seismic data processing. Although 2-D digital filters can be simulated on a general purpose computer, for applications involving high data rate, such as real time image processing, dedicated computing structures are needed in order to meet the high throughput demands. Networks using structures such as systolic arrays are popular candidates for VLSI ASIC implementation due to the regularity and modularity of the processing elements involved. Having local data communication (without global broadcast of signals) among the elements is important in such VLSI designs. In Van (2002) and Khoo et al. (2009), 2-D systolic digital filter architectures were presented which eliminated the global broadcast of the input and output signals in previous architectures (Sid-Ahmed 1989; Sunder et al. 1990). In addition, in Khoo et al. (2009), new structures realizing transfer functions with separable denominators and having diagonal magnitude symmetry were presented. It is well know that symmetry in the filter response can be used to reduce the number of multipliers in the filter realization. Recently in Chen et al. (2011), eight symmetry filter structures were presented. This creates the motivation for this work to develop a generalized formulation of the filter structures with symmetry as well as delta operator based filter structures.

In this paper, a generalized formulation is presented that allows the derivation of new 2-D VLSI filter structures, without global broadcast, using different filter sub-blocks and different interconnections/frameworks (Khoo et al. 2010). The structures include traditional z-domain filters and delta operator based filters. The delta discrete-time operator was introduced by Middleton and Goodwin in 1990. By replacing the conventional shift operator (q) in the z-domain approach with the delta discrete-time operator (δ), one can overcome the numerical ill-conditioning and coefficient sensitivity problems faced by the conventional z-domain filters when the filter poles are clustered near $z=1$. It is interesting to note that the delta operator based design approach use the same integrators as in Bruton and Strecker (1983) approach for 2-D filters and Agarwal and Burrus (1975) method for 1-D recursive filters studied in z-domain.

We start by discussing the nature of 2-D filter transfer functions and symmetry in Sects. 2 and 3 for z-domain and delta operator formulations. Then in Sect. 4, the various 1-D sub-blocks used in the 2-D filter structures are presented. Here, a general digital two-pair approach is used to describe the sub-blocks which consist of direct-form or lattice-type FIR filter in one of the frequency variables. Then, by applying the sub-blocks in various frameworks, 2-D structures realizing different transfer functions are obtained for z-domain and delta operator based filters. The structures presented in Van (2002), Khoo et al. (2009), Chen et al. (2011) are among a few of the many possible structures that can be derived using this general formulation.

Section 5 discusses the filter frameworks for realizing general IIR and FIR transfer functions. Section 6 presents the frameworks for IIR transfer functions with separable denominators where the structures exhibit the denominator separability as a filter structural property, which have important symmetry applications. Then, in Sect. 7, the filter frameworks for realizing transfer functions with quadrantal magnitude symmetry are presented. Following this, the multiplier savings for the separable denominator and symmetry structures are discussed. Then, the roundoff noise is compared among some of the representative structures. Finally, some limitations of having exact symmetry with separable 1-D denominator factors are discussed.

2 z-domain 2-D filters and symmetry

A general 2-D z-domain IIR transfer function can be represented as in (1), where $b_{00} = 0$, $N_1 \times N_2$ is the order of the filter, and X and Y are respectively the input and output of the filter. The equation can also represent an FIR transfer function if we set $b_{ij} = 0$ for all i and j.

$$H(z_1, z_2) = \frac{Y(z_1, z_2)}{X(z_1, z_2)} = \frac{\sum_{i=0}^{N_1} \sum_{j=0}^{N_2} a_{ij} z_1^{-i} z_2^{-j}}{1 - \sum_{i=0}^{N_1} \sum_{j=0}^{N_2} b_{ij} z_1^{-i} z_2^{-j}} \tag{1}$$

The usefulness of symmetry relations in the design of 2-D filters have been studied extensively (Rajan and Swamy 1978; Aly and Fahmy 1981; George and Venetsanopoulos 1984; Fettweis 1997; Reddy et al. 2003). Symmetry present in the frequency response induces a relation among the filter coefficients and multipliers. This reduces the number of design parameters in an optimization scheme, as well as the number of multipliers in an implementation structure. There are many possible types of symmetries in the magnitude response such as quadrantal, diagonal, rotational, octagonal symmetries etc. In this paper, we will focus on quadrantal symmetry.

If $P(z_1, z_2)$ is a 2-D z-domain polynomial, its frequency response is given by $P\left(e^{j\theta_1}, e^{j\theta_2}\right)$. The magnitude squared function of the frequency response is given by:

$$\begin{aligned} F(\theta_1, \theta_2) &= \left|P\left(e^{j\theta_1}, e^{j\theta_2}\right)\right|^2 \\ &= P\left(e^{j\theta_1}, e^{j\theta_2}\right) \cdot P\left(e^{-j\theta_1}, e^{-j\theta_2}\right) \\ &= P(z_1, z_2) \cdot P\left(z_1^{-1}, z_2^{-1}\right)\Big|_{z_i = e^{j\theta_i}}, \text{ i=1,2} \end{aligned} \tag{2}$$

If the magnitude squared function possesses quadrantal symmetry, then

$$\begin{aligned} F(\theta_1, \theta_2) &= F(-\theta_1, \theta_2) \\ &= F(\theta_1, -\theta_2) \\ &= F(-\theta_1, -\theta_2), \forall(\theta_1, \theta_2) \end{aligned} \tag{3}$$

Expressing (3) in terms of the polynomial yields:

$$P(z_1, z_2) \cdot P\left(z_1^{-1}, z_2^{-1}\right) \cdot z_1^{-N_1} \cdot z_2^{-N_2} = P\left(z_1^{-1}, z_2\right) \cdot P\left(z_1, z_2^{-1}\right) \cdot z_1^{-N_1} \cdot z_2^{-N_2} \tag{4}$$

Note that the multiplication by $\cdot z_1^{-N_1} \cdot z_2^{-N_2}$ is needed so that both sides of the equations remain a polynomial in negative powers of z.

Applying the unique factorization property of 2-variable polynomials to (4), it can be seen that $P(z_1, z_2)$ should satisfy one of the following two conditions:

(i)

$$P\left(z_1, z_2\right) = k_1 \cdot P\left(z_1^{-1}, z_2\right) \cdot z_1^{-N_1} \text{ where } k_1 \text{ is a real constant.} \tag{5}$$

(ii)

$$P\left(z_1, z_2\right) = k_2 \cdot P\left(z_1, z_2^{-1}\right) \cdot z_2^{-N_2} \text{ where } k_2 \text{ is a real constant.} \tag{6}$$

Each of the above condition will provide the constraint on the polynomial for it to possess quadrantal symmetry in its magnitude response.

Substituting $P\left(z_1, z_2\right) = \sum_{i=0}^{N_1} \sum_{j=0}^{N_2} a_{ij} \cdot z_1^{-i} \cdot z_2^{-j}$ into condition (i) above and assuming $k_1=1$, we get:

$$\sum_{i=0}^{N_1} \sum_{j=0}^{N_2} a_{ij} \cdot z_1^{-i} \cdot z_2^{-j} = \sum_{i=0}^{N_1} \sum_{j=0}^{N_2} a_{ij} \cdot z_1^{i-N_1} \cdot z_2^{-j} \tag{7}$$

Applying a change of variable $i' = N_1 - i$ to (7), we obtain:

$$\sum_{i=0}^{N_1} \sum_{j=0}^{N_2} a_{ij} \cdot z_1^{-i} \cdot z_2^{-j} = \sum_{i'=0}^{N_1} \sum_{j=0}^{N_2} a_{N_1-i',j} \cdot z_1^{-i'} \cdot z_2^{-j} \tag{8}$$

So the coefficient constraint $a_{ij} = a_{N_1-i,j}$ will ensure that the polynomial $P\left(z_1, z_2\right)$ possesses quadrantal symmetry in its magnitude response.

The same steps can be applied to condition (ii) above to obtain another coefficient constraint $a_{ij} = a_{i,N_2-j}$ for quadrantal symmetry.

These coefficient constraints can be applied to the transfer function of an FIR filter to ensure quadrantal symmetry. For an IIR filter, the constraint can be applied to the numerator polynomial. The denominator can be selected as separable, i.e. $P_1\left(z_1\right) \cdot P_2\left(z_2\right)$. It is easy to see that $P_1\left(z_1\right)$ satisfies $a_{ij} = a_{i,N_2-j}$ and $P_2\left(z_2\right)$ satisfies $a_{ij} = a_{N_1-i,j}$, so their product possesses quadrantal symmetry. In addition, because the denominator is separable, it is easy to check the stability.

The symmetry constraints can be used to obtain filter structures with fewer number of multipliers which will be discussed in a later section.

3 Delta operator formulation

Conventional discrete time filters and systems utilizing the shift operator (q) in z-domain can exhibit unacceptable numerical problems when the filter is narrowband or when the filter poles are clustered near z = 1 in the complex z-plane, such as when high sampling rates are needed (Middleton and Goodwin 1990; Goodwin et al. 1992). This translates into very poor coefficient and filter parameter sensitivity. By replacing the conventional shift operator (q) in the z-domain approach with the delta discrete-time operator (δ), one can overcome this numerical ill-conditioning. Since the introduction by Middleton and Goodwin, delta operator based designs have been studied extensively in the area of digital control systems and signal processing due to their excellent finite wordlength performance under fast sampling (Premaratne et al. 1994; Kauraniemi et al. 1998; Wong and Ng 2000). The delta operator is defined as:

$$\delta\left[x\left(nT\right)\right] = \frac{x\left(nT+T\right) - x\left(nT\right)}{T} \tag{9}$$

where T may denote the sampling period or a constant.

It is easy to see that the relationship between the delta operator and the shift operator is given by $\delta = (q-1)/T$. In the transform domain, δ is represented by the transform variable $\gamma = (z-1)/T$. Or, as a causal element: $\gamma^{-1} = T \cdot z^{-1}/\left(1 - z^{-1}\right)$. Following the notations in Khoo et al. (2006), let $\gamma_i = (z_i - 1)/T_i$ for $i = 1, 2$, represent the delta operator in the transform domain for 2-D systems. Then the transfer functions of a 2-D system $H(z_1, z_2)$ in the z-domain and $H_\gamma(\gamma_1, \gamma_2)$ in the γ-domain are related as follows:

$$H_\gamma(\gamma_1, \gamma_2) = H(z_1, z_2)|_{z_i=(1+T_i\gamma_i),\quad i=1,2} \tag{10}$$

and

$$H(z_1, z_2) = H_\gamma(\gamma_1, \gamma_2)\Big|_{\gamma_i=\frac{(z_i-1)}{T_i},\quad i=1,2} \tag{11}$$

where

$$H_\gamma(\gamma_1, \gamma_2) = \frac{Y(\gamma_1, \gamma_2)}{X(\gamma_1, \gamma_2)} = \frac{\sum_{i=0}^{N_1}\sum_{j=0}^{N_2} c_{ij}\gamma_1^{-i}\gamma_2^{-j}}{1 - \sum_{i=0}^{N_1}\sum_{j=0}^{N_2} d_{ij}\gamma_1^{-i}\gamma_2^{-j}} \tag{12}$$

If $P_\gamma(\gamma_1, \gamma_2)$ is a 2-D γ-domain polynomial, then its frequency response is given by $P_\gamma\left(\frac{e^{j\theta_1}-1}{T}, \frac{e^{j\theta_2}-1}{T}\right)$. The magnitude squared function of the frequency response is given by:

$$\begin{aligned} F(\theta_1, \theta_2) &= P_\gamma\left(\frac{e^{j\theta_1}-1}{T}, \frac{e^{j\theta_2}-1}{T}\right) \cdot P_\gamma\left(\frac{e^{-j\theta_1}-1}{T}, \frac{e^{-j\theta_2}-1}{T}\right) \\ &= P_\gamma(\gamma_1, \gamma_2) \cdot P_\gamma\left(\frac{-\gamma_1}{1+T\gamma_1}, \frac{-\gamma_2}{1+T\gamma_2}\right)\Bigg|_{\gamma_i=\frac{e^{j\theta_i}-1}{T},\quad i=1,2} \end{aligned} \tag{13}$$

Following the same procedure in the z-domain discussion, it can be shown that in order for $P_\gamma(\gamma_1, \gamma_2)$ to possess quadrantal symmetry in its magnitude squared response, it should satisfy one of the following two conditions:

(i)

$$P_\gamma(\gamma_1, \gamma_2) = k_1 \cdot P_\gamma\left(\frac{-\gamma_1}{1+T\gamma_1}, \gamma_2\right) \text{ where } k_1 \text{ is a real constant.} \tag{14}$$

(ii)

$$P_\gamma(\gamma_1, \gamma_2) = k_2 \cdot P_\gamma\left(\gamma_1, \frac{-\gamma_2}{1+T\gamma_2}\right) \text{ where } k_2 \text{ is a real constant.} \tag{15}$$

Unlike z-domain, the coefficient symmetry constraints here do not result in a simple relationship. So a symmetry constraint based on the polynomial form will be used instead. To do that, we first observe that the term $\gamma_i^{-2} + T\gamma_i^{-1}$ is self inverse in γ_i. That is:

$$\gamma_i^{-2} + T\gamma_i^{-1}\Big|_{\gamma_i=\frac{-\gamma_i}{1+T\gamma_i}} = \gamma_i^{-2} + T\gamma_i^{-1}$$

Therefore, polynomials of the form $P_\gamma\left(\gamma_1^{-2} + T\gamma_1^{-1}, \gamma_2\right)$ and $P_\gamma\left(\gamma_1, \gamma_2^{-2} + T\gamma_2^{-1}\right)$ satisfies (14) and (15) respectively. This means that polynomials that can be expressed in terms of $\gamma_1^{-2} + T\gamma_1^{-1}$ or $\gamma_2^{-2} + T\gamma_2^{-1}$ will possess quadrantal symmetry (Note that we will assume $T = 1$ in the discussion that follows). These polynomial forms will be used in the numerator of the delta operator IIR filter transfer function with quadrantal symmetry. However, they cannot be used for the denominator due to stability problem. Instead, the denominator is chosen as separable, i.e. $P_{1\gamma}(\gamma_1) \cdot P_{2\gamma}(\gamma_2)$. It is easy to see that $P_{1\gamma}(\gamma_1)$ and $P_{2\gamma}(\gamma_2)$ satisfies (15) and (14) respectively, so their product possesses quadrantal symmetry. Again, the advantage of a separable denominator is that it is easy to ensure the stability.

4 Filter sub-blocks

The z-domain transfer function in (1) can also be expressed as:

$$H(z_1, z_2) = \frac{\sum_{i=0}^{N_1} F_i(z_2) \cdot z_1^{-i}}{1 - \sum_{i=0}^{N_1} G_i(z_2) \cdot z_1^{-i}} \tag{16}$$

where $F_i(z_2) = \sum_{j=0}^{N_2} a_{ij} z_2^{-j}$ and $G_i(z_2) = \sum_{j=0}^{N_2} b_{ij} z_2^{-j}$ are 1-D FIR functions in z_2 variable only. These 1-D functions can be realized by the general digital two-pair networks depicted as sub-blocks here. The sub-blocks can be lattice or direct form structures. These sub-blocks are then used in the filter frameworks in Sect. 5 to realize the overall 2-D transfer function in (16).

In our discussion, we assume that the filter is used to process a square image of size M×M and the pixel values in the image are fed to the filter in raster-scan mode, i.e. the input sequence is x(0,0), x(0,1), …, x(0,M−1), x(1,0), x(1,1), … etc. We can then replace z_2^{-1} by a single delay register, z^{-1}, and z_1^{-1} by a shift register of length M, z^{-M}, provided $M > N_2$. Without loss of generality, we will assume $N_1 = N_2 = N$ in discussing the filters.

Sub-block #1, shown in Fig. 1, has 2 inputs and 1 output. It is direct form, i.e. the multiplier values are the same as the polynomial coefficients. It realizes the following two FIR functions:

$$F_i\left(z^{-1}\right) = \left.\frac{Y_i}{X_i}\right|_{W_i=0} = \sum_{j=0}^{N} a_{ij} z^{-j}\ ,\ G_i\left(z^{-1}\right) = \left.\frac{Y_i}{W_i}\right|_{X_i=0} = \sum_{j=0}^{N} b_{ij} z^{-j} \tag{17}$$

Note that the special arrangement of the delays is to eliminate global broadcast of the signals, X_i and W_i, and also to control the critical period. The critical period is the time required for the signal through the slowest (critical) path of the structure and determines the highest possible clock speed of the structure.

Sub-block #2 is shown in Fig. 2. It has 1 input and 2 outputs and realizes the following two FIR functions. It is also direct form. It can be used to realize the 2-D transfer function in (16) with E_i and D_i replacing F_i and G_i respectively. The filter framework to achieve this will be discussed in the next section.

$$D_i\left(z^{-1}\right) = \frac{V_i}{X_i} = \sum_{j=0}^{N} b_{ij} z^{-j},\ E_i\left(z^{-1}\right) = \frac{Y_i}{X_i} = \sum_{j=0}^{N} a_{ij} z^{-j} \tag{18}$$

The alternate lattice form for sub-block#2 is shown in Fig. 3. Unlike a regular lattice, this structure has different multipliers in the top and bottom branches. The algorithm to extract the multipliers A, B, k_{aij}, k_{bij} is as follows:

Step 1: Let $P_{iN} = E_i$ and $Q_{iN} = D_i$; $j = N$

Step 2: $k'_{bij} = \dfrac{\text{coefficient of } z^{-j} \text{ term in } Q_{ij}}{\text{coefficient of } z^{-j} \text{ term in } P_{ij}}$ and $k'_{aij} = \dfrac{\text{constant term in } P_{ij}}{\text{constant term in } Q_{ij}}$

Step 3: $P_{i(j-1)} = \dfrac{k'_{bij} \cdot P_{ij} - Q_{ij}}{k'_{aij} \cdot k'_{bij} - 1}$ and $Q_{i(j-1)} = \dfrac{P_{ij} - k'_{aij} \cdot Q_{ij}}{z^{-1} \cdot \left(1 - k'_{aij} \cdot k'_{bij}\right)}$

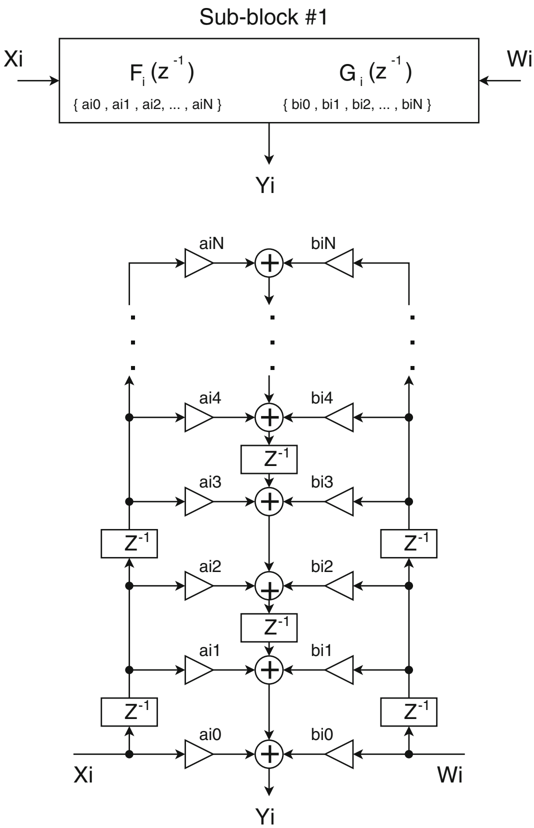

Fig. 1 Sub-block #1 (2-inputs-1-outputs, direct-form)

Step 4: $j = j - 1$. If $j \neq 0$, go back to Step 2.
Step 5: If N is even, $A = P_{i0}$ and $B = Q_{i0}$. Otherwise, $A = Q_{i0}$ and $B = P_{i0}$.
Step 6: $k_{bij} = k'_{bij} \cdot \frac{A}{B}$ and $k_{aij} = k'_{aij} \cdot \frac{B}{A}$ for all even (N-j).
$k_{bij} = k'_{bij} \cdot \frac{B}{A}$ and $k_{aij} = k'_{aij} \cdot \frac{A}{B}$ for all odd (N-j).

Like a regular lattice, the structure cannot realize functions where the constant term is zero, i.e. ai0 = 0 or bi0 = 0. Also note the extra delays (circled in Fig. 3) added to control the critical period. This will result in latency in the form of extra z^{-1} factors in (18). However, the factors can be cancelled in the final reconfiguration to be discussed in Sect. 5 so that the overall 2-D transfer function will not have any latency. The lattice-form in Fig. 3 has the same number of multipliers and adders as the direct-form in Fig. 2. It does, however, require more delay elements.

Another z-domain sub-block is sub-block #3. The direct-form version is shown in Fig. 4. The alternating delay arrangement is to eliminate global broadcast of the signal X_i and to control the critical period. The sub-block has 1 input and 1 output and realizes the FIR function in (19). Note that ρ_{ij} can represent either the numerator or denominator coefficient a_{ij} or b_{ij}.

Fig. 2 Sub-block #2 (1-input-2-outputs, direct-form)

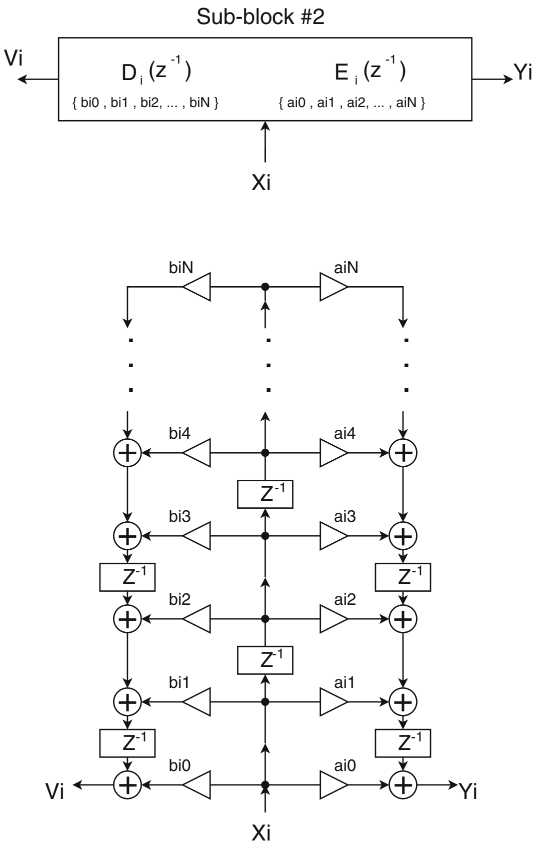

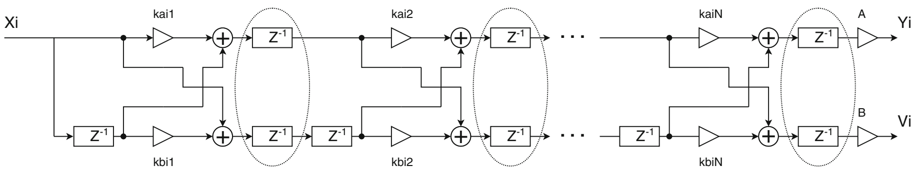

Fig. 3 Sub-block #2 (1-input-2-outputs, lattice-form)

$$C_{\rho i}\left(z^{-1}\right)=\frac{Y_i}{X_i}=\sum_{j=0}^{N}\rho_{ij}z^{-j} \tag{19}$$

The lattice version of sub-block #3 is shown in Fig. 5. This is based on the one-multiplier lattice in Makhoul (1978). The multiplier values, k_{ij}, can be determined from the function coefficients a_{ij}, using the regular lattice extraction plus appropriate scaling of the results (Makhoul 1978). Note that extra delays (in circle) are added to control the critical period, which will result in latency in the form of z^{-1} factor in (19). The latency can be removed in the filter framework to be discussed in Sect. 5. One limitation of the structure is that it cannot

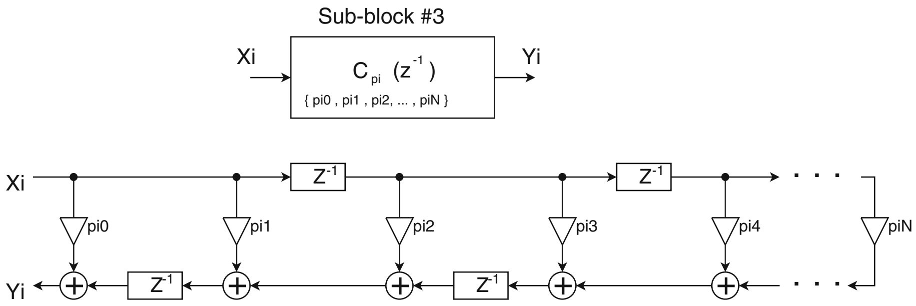

Fig. 4 Sub-block #3 (1-input-1-output, direct-form)

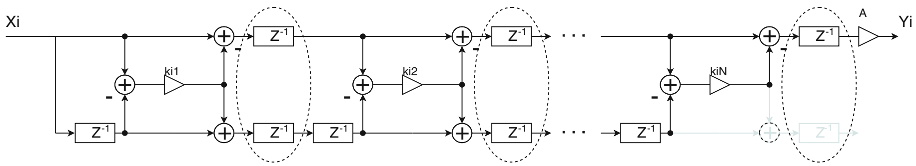

Fig. 5 Sub-block #3 (1-input-1-output, lattice-form)

realize functions where $\rho i0 = 0$. Also, compared to direct-form, the lattice version requires more delays and adders, but the number of multipliers is the same.

For the delta operator formulation, the transfer function in (12) can also be expressed as:

$$H_\gamma(\gamma_1, \gamma_2) = \frac{\sum_{i=0}^{N_1} F_i^g(\gamma_2) \cdot \gamma_1^{-i}}{1 - \sum_{i=0}^{N_1} G_i^g(\gamma_2) \cdot \gamma_1^{-i}} \tag{20}$$

where $F_i^g(\gamma_2) = \sum_{j=0}^{N_2} c_{ij}\gamma_2^{-j}$ and $G_i^g(\gamma_2) = \sum_{j=0}^{N_2} d_{ij}\gamma_2^{-j}$ are 1-D polynomials in γ_2 to be realized by the sub-blocks discuss here. In the sub-blocks, we represent γ_2^{-1} by γ^{-1}. γ_1^{-1} will be realized by a delta operator shift register, to be discussed in the next section. Again, we will assume $N_1 = N_2 = N$ in discussing the filters.

The sub-blocks #4 and #5 for use in the delta-operator realization are shown in Figs. 6 and 7 respectively. The $z^{-1}/1$ element inside can be configured to either implement a delay or a passthrough. This allows the sub-blocks to realize either a regular polynomial or quadrantal symmetry polynomial.

In the diagrams, the g^{-1} and zg^{-1} elements are equivalent to $\gamma^{-1} = \frac{z^{-1}}{1-z^{-1}}$ and $z.\gamma^{-1} = z \cdot \frac{z^{-1}}{1-z^{-1}} = \frac{1}{1-z^{-1}}$ respectively. They can be implemented as shown in Figs. 8 and 9. Note that the cascade connection of the g^{-1} and zg^{-1} elements yields the self inverse term $\left(\gamma^{-2} + \gamma^{-1}\right)$ needed for quadrantal symmetry, i.e. $z \cdot \gamma^{-2} = (1+\gamma).\gamma^{-2} = \left(\gamma^{-2} + \gamma^{-1}\right)$.

Sub-block #4 in Fig. 6 has 2 inputs and 1 output. With the $z^{-1}/1$ element configured as a delay, it realizes the following two polynomial functions:

$$F_i^g\left(\gamma^{-1}\right) = \left.\frac{Y_i}{X_i}\right|_{W_i=0} = \sum_{j=0}^{N} c_{ij}\gamma^{-j},\ G_i^g\left(\gamma^{-1}\right) = \left.\frac{Y_i}{W_i}\right|_{X_i=0} = \sum_{j=0}^{N} d_{ij}\gamma^{-j} \tag{21}$$

Fig. 6 Sub-block #4 (2-inputs-1-output, delta operator direct form)

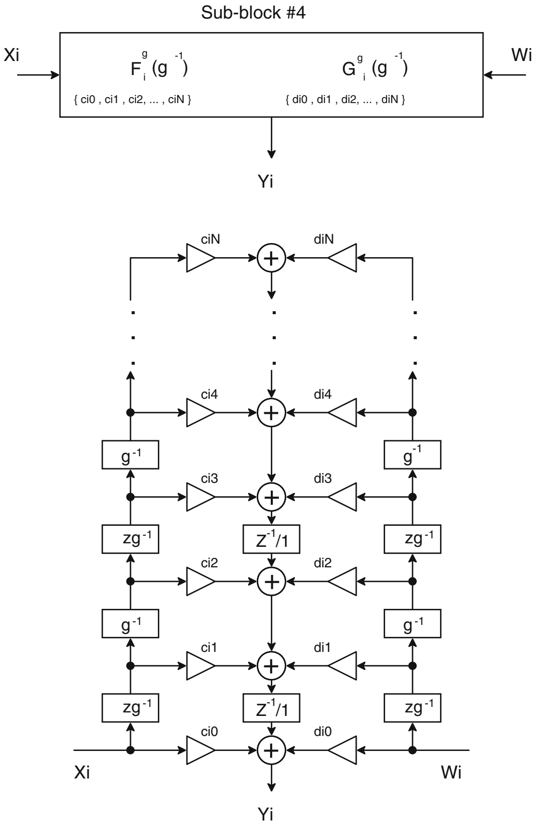

With the $z^{-1}/1$ element configured as a passthrough and with $c_{ij} = 0, d_{ij} = 0$ for $j = 1,3,5\ldots$, it realizes the following functions, which can be used for quadrantal symmetry.

$$
\begin{aligned}
F_i^g\left(\gamma^{-1}\right) &= \left.\frac{Y_i}{X_i}\right|_{W_i=0} = c_{i0} + c_{i2}\left(z\cdot\gamma^{-2}\right) + c_{i4}\left(z\cdot\gamma^{-2}\right)^2 + \cdots \\
&= \sum_{j=0,2,4\ldots}^{N} c_{ij}\left(z\cdot\gamma^{-2}\right)^{\frac{j}{2}} \\
&= \sum_{j=0,2,4\ldots}^{N} c_{ij}\left(\gamma^{-2}+\gamma^{-1}\right)^{\frac{j}{2}}
\end{aligned} \tag{22}
$$

$$
\begin{aligned}
G_i^g\left(\gamma^{-1}\right) &= \left.\frac{Y_i}{W_i}\right|_{X_i=0} = d_{i0} + d_{i2}\left(z\cdot\gamma^{-2}\right) + d_{i4}\left(z\cdot\gamma^{-2}\right)^2 + \cdots \\
&= \sum_{j=0,2,4\ldots}^{N} d_{ij}\left(z\cdot\gamma^{-2}\right)^{\frac{j}{2}} \\
&= \sum_{j=0,2,4\ldots}^{N} d_{ij}\left(\gamma^{-2}+\gamma^{-1}\right)^{\frac{j}{2}}
\end{aligned}
$$

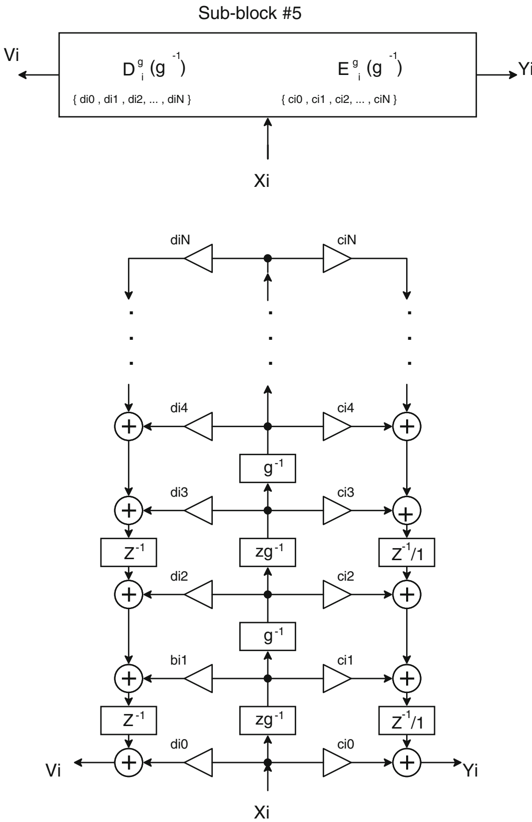

Fig. 7 Sub-block #5 (1-input-2-outputs, delta operator direct form)

Fig. 8 Realization of γ^{-1}

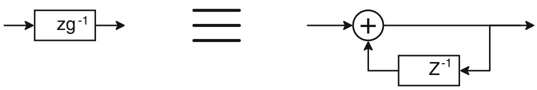

Fig. 9 Realization of $z.\gamma^{-1}$

The other delta operator sub-block is Sub-block #5 (Fig. 7) which has 1 input and 2 outputs. It realizes the following two polynomial functions with the $z^{-1}/1$ element configured as a delay:

$$D_i^g\left(\gamma^{-1}\right) = \frac{V_i}{X_i} = \sum_{j=0}^{N} d_{ij}\gamma^{-j},\ E_i^g\left(\gamma^{-1}\right) = \frac{Y_i}{X_i} = \sum_{j=0}^{N} c_{ij}\gamma^{-j} \tag{23}$$

Sub-block #5 can be used to realize the 2-D transfer function in (20) with E_i^g and D_i^g replacing F_i^g and G_i^g respectively. The filter framework to achieve this will be discussed in the next section.

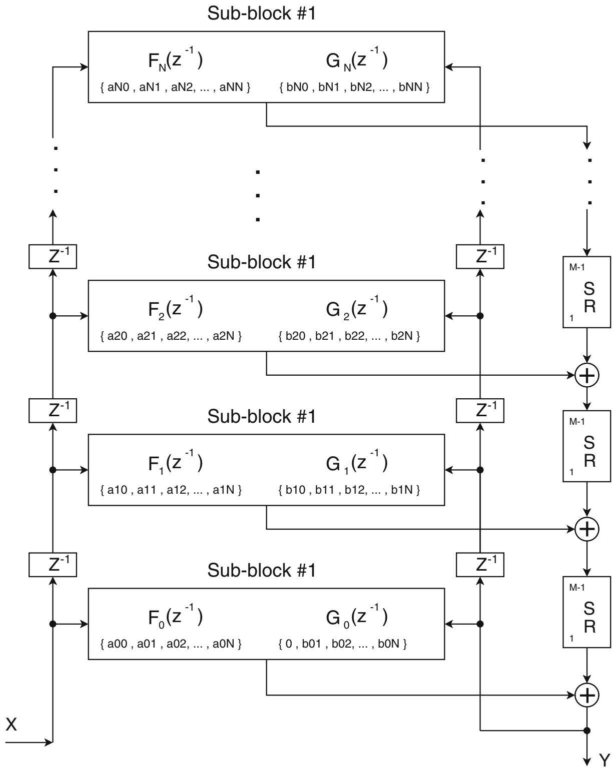

Fig. 10 Filter framework A (IIR)

With the $z^{-1}/1$ element configured as a passthrough and with $c_{ij} = 0, d_{ij} = 0$ for $j = 1,3,5\ldots$, the sub-block realizes the following functions, which can be used for quadrantal symmetry.

$$D_i^g\left(\gamma^{-1}\right) = \frac{V_i}{X_i} = \sum_{j=0,2,4\ldots}^{N} d_{ij}\left(\gamma^{-2}+\gamma^{-1}\right)^{\frac{j}{2}} \tag{24}$$

$$E_i^g\left(\gamma^{-1}\right) = \frac{Y_i}{X_i} = \sum_{j=0,2,4\ldots}^{N} c_{ij}\left(\gamma^{-2}+\gamma^{-1}\right)^{\frac{j}{2}} \tag{25}$$

The frameworks to achieve the delta operator transfer functions will be discussed in the next section.

5 Filter frameworks for realizing general transfer function

The sub-blocks discussed in the previous section are used in the filter frameworks in this section to realize the general 2-D z-domain transfer function in (1) and the delta operator transfer function in (12).

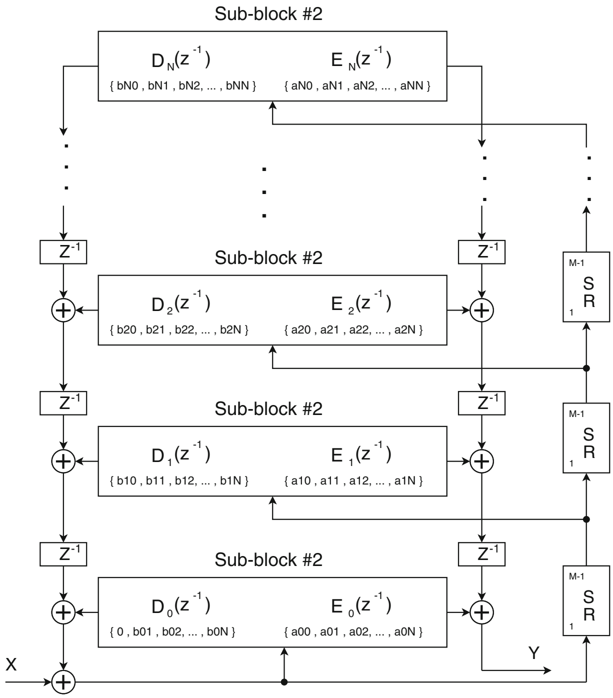

Fig. 11 Filter framework B (IIR)

Filter framework A is shown in Fig. 10. It uses only filter sub-block #1. Notice that the shift registers (SR) are of length M-1 due to the additional delays added at the input and output branches to eliminate the global broadcast. It can be verified using Mason's gain formula that the structure, with $z^{-1} = z_2^{-1}$ and SR $= z_1^{-1}z_2$, possesses the transfer function in (16).

Filter framework B is shown in Fig. 11. It utilizes sub-block #2 and realizes the 2-D transfer function in (16) with the notation change from F_i and G_i to E_i and D_i respectively, which highlights the difference in sub-blocks. Filter framework B is the transpose of filter framework A.

As discussed in Sect. 4, there are two versions of sub-block #2—direct-form (Fig. 2) and lattice-form (Fig. 3). They can be used in any combination in the framework. The only restriction is that the bottom sub-block has to be direct-form. The reason is that the lattice-form cannot realize a function where the constant term is zero, as is needed for function D_0. Also, if the lattice-forms are used (which introduce a latency of z_2^{-N}), the length of the SR can be adjusted to compensate for the latency so that the overall 2-D transfer function will not have any latency. For instance, if the bottom sub-block is direct-form while the rest are lattice, then the bottom SR will need to be of length M−N−1 (realizing $z_1^{-1}z_2^{N+1}$) rather than M−1 (realizing $z_1^{-1}z_2$).

Filter framework C is shown in Fig. 12. It uses only sub-block #3, either the direct-form of Fig. 4 or the lattice-form of Fig. 5. It realizes the 2-D transfer function in (16) with the notation change from F_i to C_{ai} and from G_i to C_{bi} . Note that the direct and lattice-form sub-blocks can be used in any combination in the framework. The only restriction is that the C_{b0} sub-block needs to be direct-form as the lattice-type cannot realize a function with a zero constant term. Once again, if the lattice-forms are used, appropriate adjustments can be

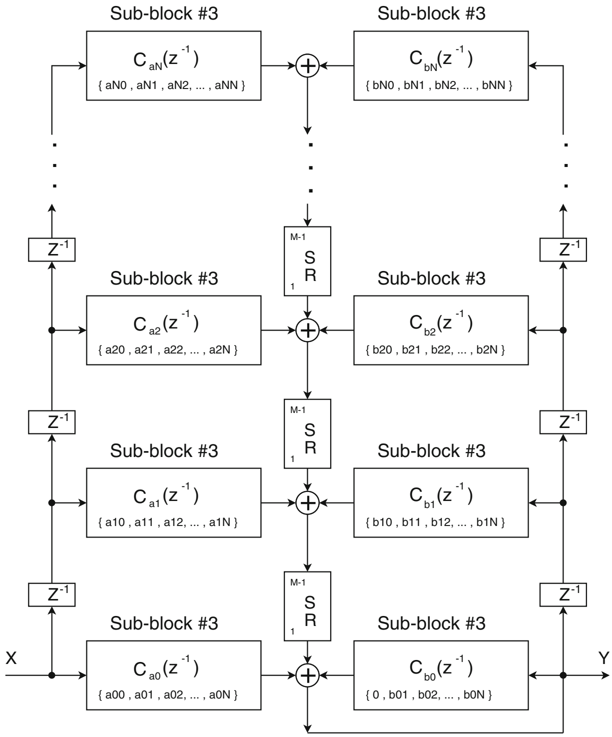

Fig. 12 Filter framework C (IIR)

made to the SR to avoid the latency. Filter framework D, shown in Fig. 13, is the transpose of framework C.

To realize 2-D FIR transfer functions, the C_{bi} sub-blocks may be removed in frameworks C or D above. This yields framework E as shown in Fig. 14.

Filter framework J in Fig. 15 can be used to realize the 2-D delta operator transfer function in (20) with E_i^g and D_i^g replacing F_i^g and G_i^g respectively. It uses sub-block #5. The $Z^{-1}/1$ elements in sub-block #5 are configured as delays. Note that the delta operator shift register (gSR), which realizes $z \cdot \gamma_1^{-1}$, is implemented as shown in Fig. 16. It consists of a regular shift register with a loop and delay around it. Note that the transpose of filter framework J is not presented as it has noise problem. Also, there is no polynomial form delta operator FIR filter.

6 Filter frameworks for realizing transfer functions with separable denominator

By mixing the sub-blocks in specific ways, filter frameworks realizing transfer functions with separable denominator of the form in (26) can be obtained. The idea is to form two non-touching loops in different variables as per Mason's gain formula.

$$H(z_1, z_2) = \frac{Y(z_1, z_2)}{X(z_1, z_2)} = \frac{\sum_{i=0}^{N_1} \sum_{j=0}^{N_2} a_{ij} z_1^{-i} z_2^{-j}}{\left(1 - \sum_{i=1}^{N_1} b_{i0} z_1^{-i}\right) \cdot \left(1 - \sum_{j=1}^{N_2} b_{0j} z_2^{-j}\right)} \tag{26}$$

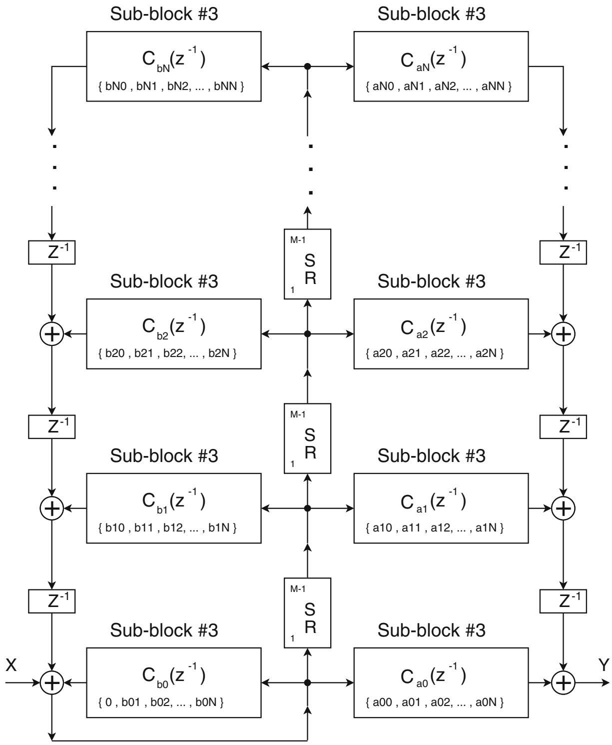

Fig. 13 Filter framework D (IIR)

The significant feature of these structures is that they exhibit the denominator separability as a filter structural property, independent of the choice of multiplier values. The separable denominator transfer function has several advantages over the general one in (1). Firstly, the stability can be checked by simply solving for the poles of the two 1-D polynomials, and any unstable pole is easy to stabilize. Secondly, the separable denominator requires fewer multipliers to realize. Thirdly, the separable denominator is required in realizing stable magnitude responses possessing various symmetries such as quadrantal symmetry (Reddy et al. 2003). This was discussed in the earlier section.

Filter framework F is shown in Fig. 17. It is based on framework A. It uses sub-block #2 at the bottom while the rest are sub-block #1 (Note that the lattice-form cannot be used here). It realizes the transfer function in (27), with G_i's being constants. Recall that $z^{-1} = z_2^{-1}$ and $\mathrm{SR} = z_1^{-1} z_2$.

$$\frac{Y}{X} = \frac{E_0\left(z_2\right) + \sum_{i=1}^{N} F_i\left(z_2\right) \cdot z_1^{-i}}{\left[1 - D_0\left(z_2\right)\right] \cdot \left[1 - \sum_{i=1}^{N} G_i \cdot z_1^{-i}\right]} \tag{27}$$

By taking the transpose of filter framework F, framework G can be obtained. See Fig. 18. It uses sub-block #1 at the bottom of the framework while the rest are sub-block #2. It realizes the transfer function in (27) but with term Ei replacing Fi, and Di replacing Gi. It is to be noted that Type-I and Type-II separable denominator 2-D IIR filer structures in Chen et al. (2011) can be derived from framework G and framework F, respectively.

Fig. 14 Filter framework E (FIR)

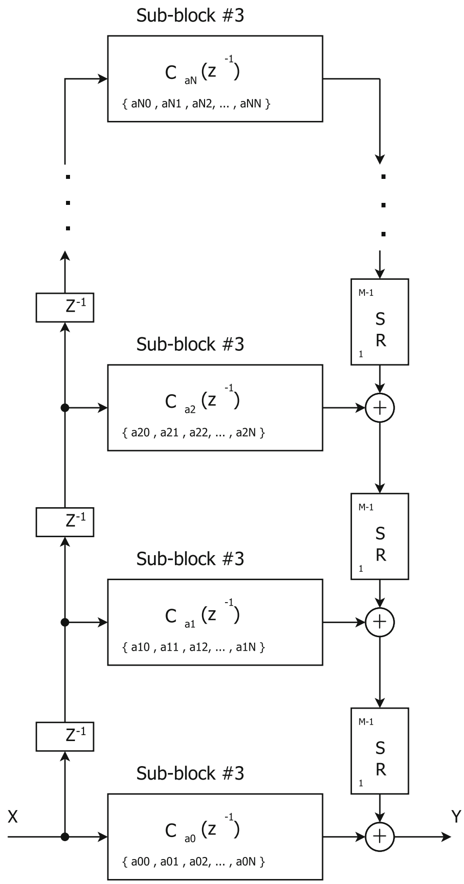

Filter framework H is shown in Fig. 19. It uses only sub-block #3. It realizes the transfer function in (27) with the terms C_{ai} replacing F_i for i = 1…N, and C_{a0} replacing E_0. Also, C_{bi} replaces D_i for i = 1…N, and C_{b0} replaces G_0 in (27). Note that the bottom two sub-blocks have reversed input-output compared to the rest of the sub-blocks. Finally, filter framework I (Fig. 20) is the transpose of framework H.

Filter framework K (Fig. 21) is used to realize the following delta operator separable denominator transfer function:

$$\frac{Y}{X} = \frac{\sum_{i=0}^{N}\sum_{j=0}^{N} c_{ij}\gamma_1^{-i}\gamma_2^{-j}}{\left(1-\sum_{i=1}^{N} d_{i0}\gamma_1^{-i}\right)\cdot\left(1-\sum_{j=1}^{N} d_{0j}\gamma_2^{-j}\right)}$$
$$= \frac{E_0^g(\gamma_2)+\sum_{i=1}^{N} F_i^g(\gamma_2)\cdot\gamma_1^{-i}}{\left[1-D_0^g(\gamma_2)\right]\cdot\left[1-\sum_{i=1}^{N} G_i^g\cdot\gamma_1^{-i}\right]} \tag{28}$$

The framework bears some similarity to the z-domain framework F. It uses sub-block #5 at the bottom while the rest are sub-block #4. The $Z^{-1}/1$ elements in sub-blocks #4 and #5 are configured as delays. Recall that $\gamma^{-1} = \gamma_2^{-1}$ and gSR $= z\cdot\gamma_1^{-1}$. By applying Mason's rule, it is easy to see that the structure satisfies (28).

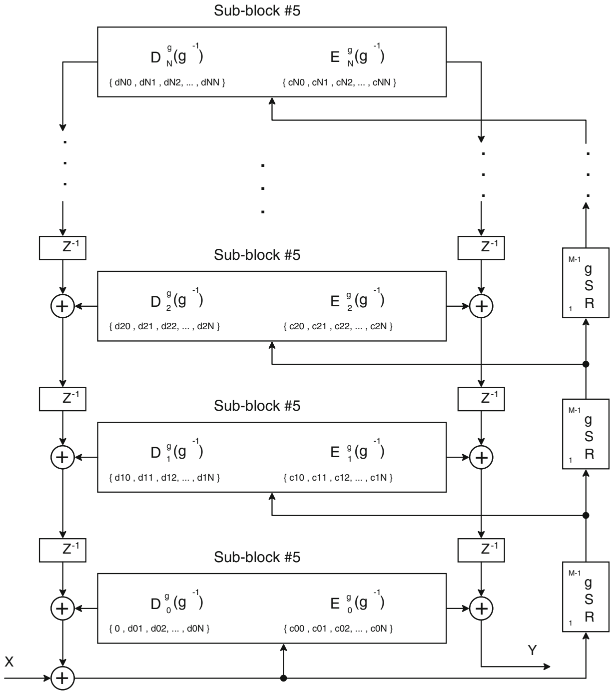

Fig. 15 Filter framework J (delta operator IIR)

Fig. 16 Implementation of delta operator shift register.

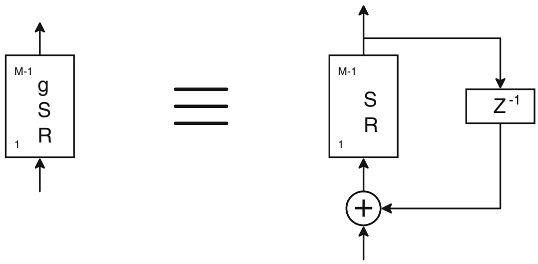

7 Quadrantal symmetry filter frameworks

The presence of symmetry in the 2-D frequency response induces certain relationship among the filter coefficients which can result in fewer multipliers in the implementation. The z-domain quadrantal symmetry coefficient constraint $a_{ij} = a_{(N-i)j}$ derived earlier can be applied to frameworks F and G to yield the new quadrantal symmetry structures as shown in Figs. 22 and 23. Note that the changes are highlighted in red, and although the structures shown are 2×2, they can easily be generalized to higher orders. As mentioned in Sect. 2, the coefficient constraint is only applied to the numerator of the IIR transfer function while the denominator is chosen as separable.

In a similar manner, the symmetry constraint can be applied to filter frameworks H and I, as well as FIR framework E, to yield new structures with the symmetry. They are shown in

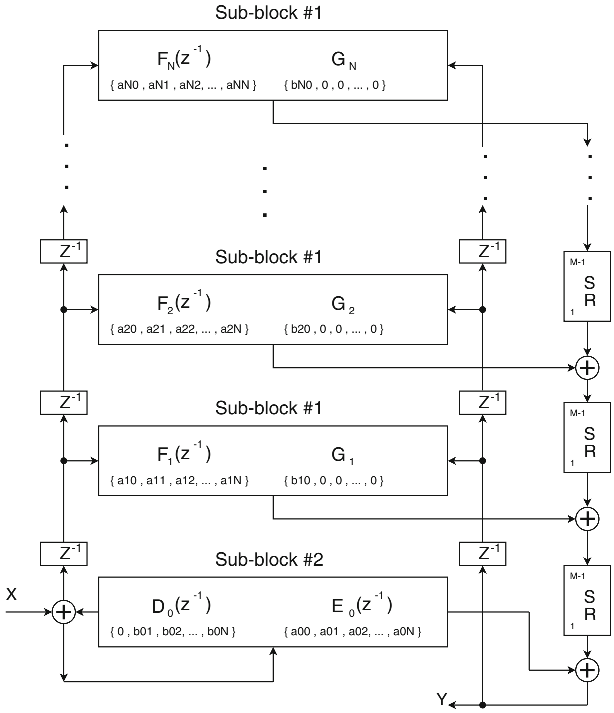

Fig. 17 Filter framework F (separable denominator)

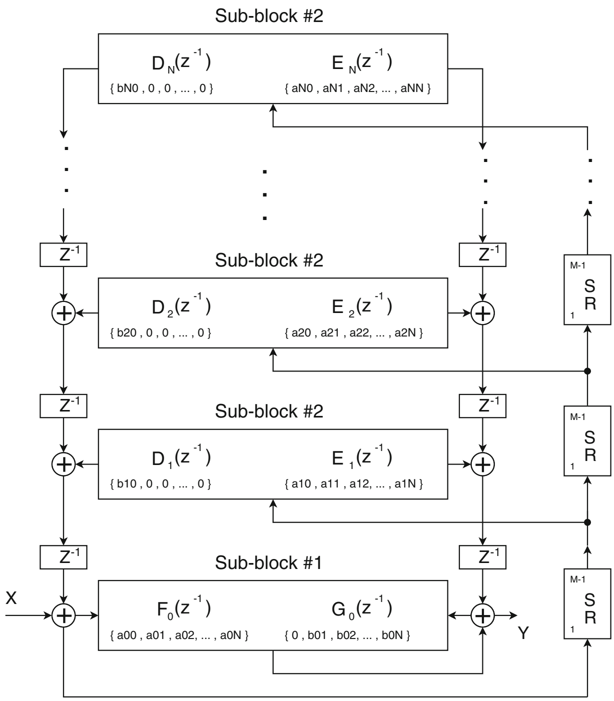

Fig. 18 Filter framework G (separable denominator)

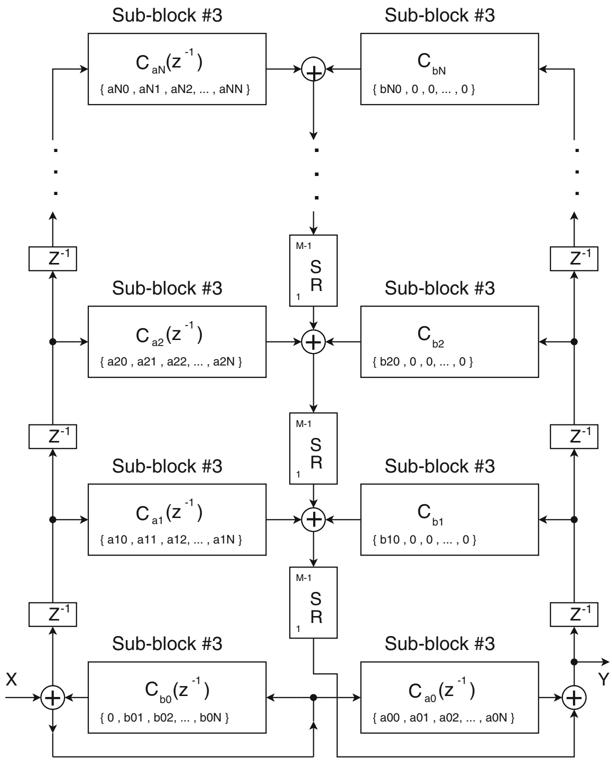

Fig. 19 Filter framework H (separable denominator)

Figs. 24, 25 and 26. It is also possible to apply the other symmetry constraint $a_{ij} = a_{i,N-j}$ to the filter frameworks, but the resulting structures are more complicated.

The delta operator filter structure with quadrantal symmetry is shown in Fig. 27. It realizes the following transfer function:

$$\frac{Y}{X} = \frac{\sum_{i=0}^{N} \sum_{j=0,2,4...}^{N} c_{ij}\gamma_1^{-i}\left(\gamma_2^{-2}+\gamma_2^{-1}\right)^{\frac{j}{2}}}{\left(1-\sum_{i=1}^{N} d_{i0}\gamma_1^{-i}\right)\cdot\left(1-\sum_{j=1}^{N} d_{0j}\gamma_2^{-j}\right)} \tag{29}$$

It is based on framework K. As mentioned in Sect. 3, the numerator is based on the quadrantal symmetry polynomial form while the denominator is chosen as separable. Note that the $Z^{-1}/1$ elements in sub-blocks #4 and #5 need to be configured as passthrough. The structure can only realize even order transfer function. Compared to the z-domain symmetry structures, the delta operator one does not require special signal routing. Only the sub-block parameters need to be changed. The changes are highlighted in red in the figure.

8 Comparison of multipliers required for the structures

The quadrantal symmetry structure has the lowest number of multipliers compared to all the other structures. The filter frameworks realizing regular 2-D IIR transfer function require

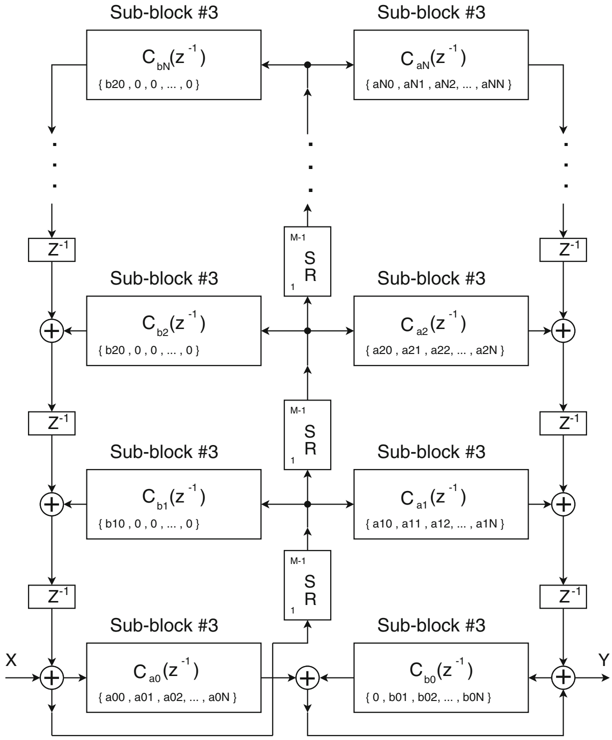

Fig. 20 Filter framework I (separable denominator)

$2(N+1)^2-1$ multipliers. The separable denominator frameworks require fewer multipliers: $(N+1)^2+2N$. The quadrantal symmetry structures require the least number of multipliers: only $(N+1)^2/2+2N$ and $(N/2+1)\cdot(N+1)+2N$ when N is odd and even respectively. For the 2-D FIR z-domain structures, the number of required multiplier is reduced from $(N+1)^2$ to $(N+1)^2/2$ (for N odd) or $(N/2+1)\cdot(N+1)$ (for N even) with quadrantal symmetry.

9 Roundoff noise

In the roundoff noise calculation, the filter is first scaled using L2 norm to prevent overflow at all the internal nodes. The total roundoff noise gain is then calculated by summing the square of the L2 norm of the transfer function from each multiplier output to the filter output. The L2 norm of a 2-D function F is determined as follows:

$$\|F(z_1, z_2)\|_2 = \sqrt{\frac{1}{\pi^2}\cdot\int_0^{\pi}\int_0^{\pi}\left|F\left(e^{j\theta_1}, e^{j\theta_2}\right)\right|^2\cdot d\theta_1\cdot d\theta_2}$$

Because of the numerous possible structures, the roundoff noise is analyzed only for some of the basic shift operator structures—filter frameworks A through D using the direct-form sub-blocks. The in-depth study on the roundoff noise will be provided in a future

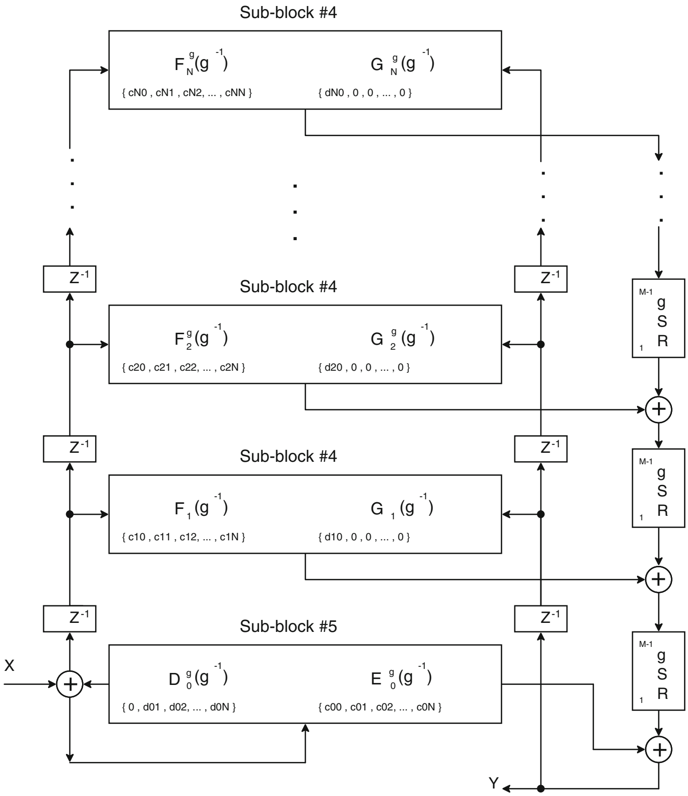

Fig. 21 Filter framework K (separable denominator, delta operator)

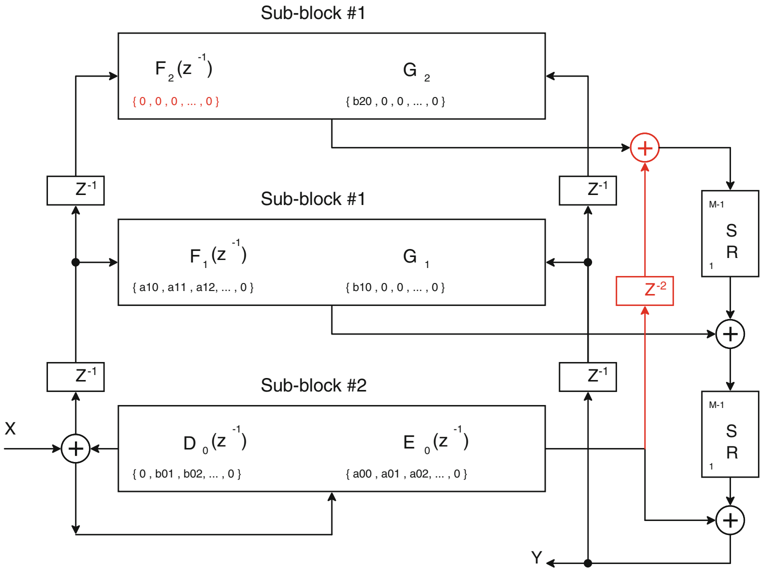

Fig. 22 Quadrantal symmetry framework based on framework F

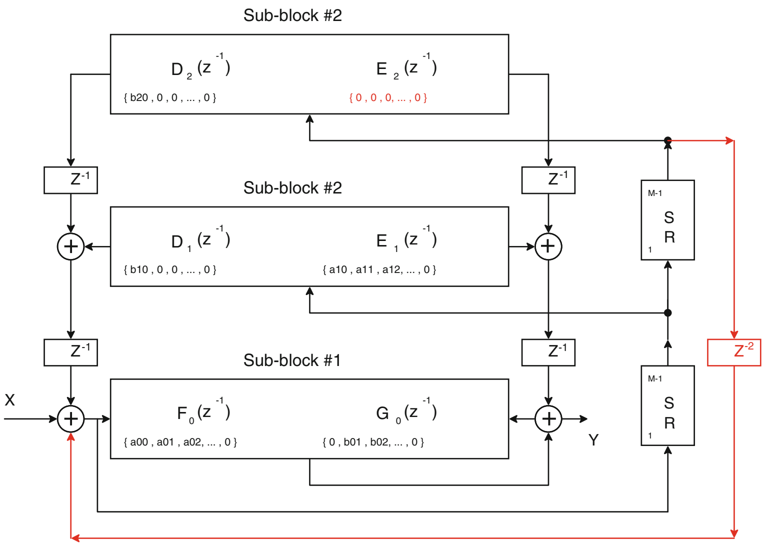

Fig. 23 Quadrantal symmetry framework based on framework G

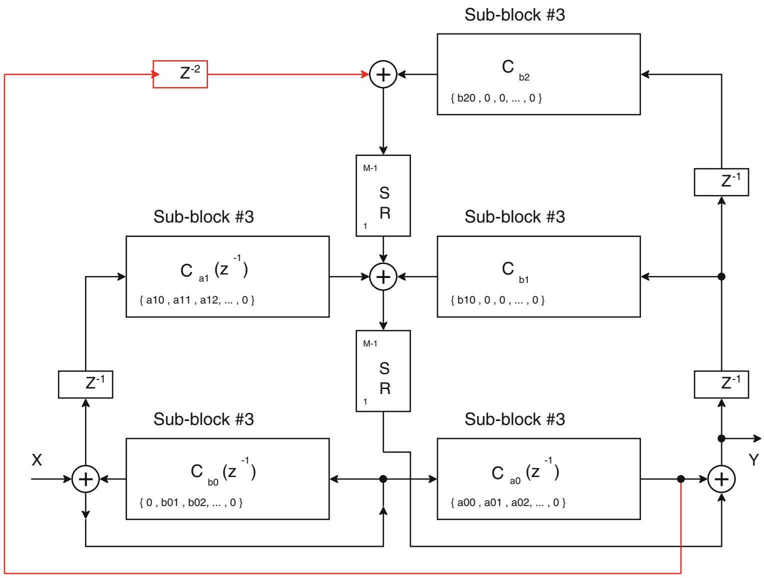

Fig. 24 Quadrantal symmetry framework based on framework H

publication. One of the selection criteria for the choice of structure may be the roundoff noise.

Assuming a 2-D lowpass filter, the roundoff noise is plotted against the filter cutoff frequency as shown in Fig. 28 for different filter orders. It can be seen that filter frameworks B and D have the lowest roundoff noise and their advantage increases with the filter order.

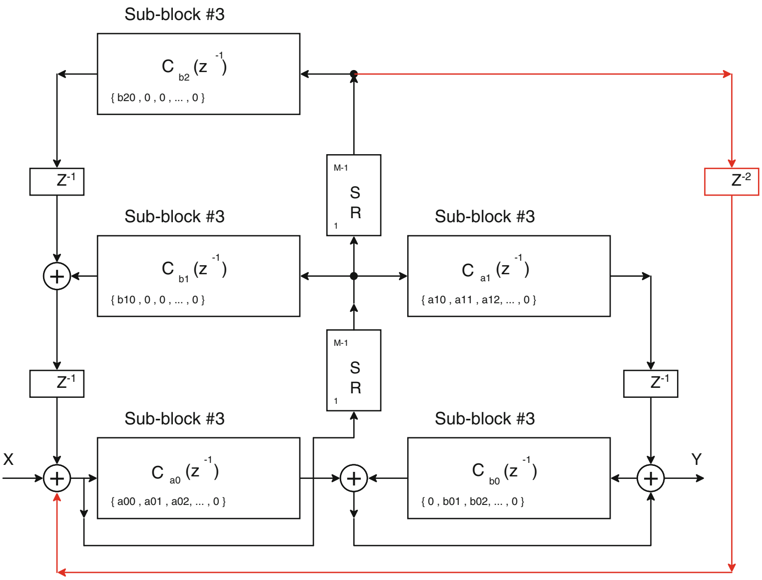

Fig. 25 Quadrantal symmetry framework based on framework I

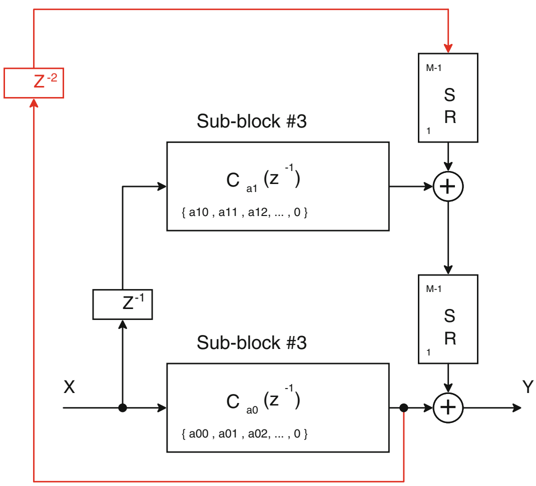

Fig. 26 Quadrantal symmetry framework based on framework E (FIR)

This is due to the fact that the noise transfer functions of frameworks B and D are bounded by one in magnitude, while those of frameworks A and C can exceed unity.

10 Some limitations of having exact symmetry with separable 1-D denominator factors

As stated earlier, for a 2-D digital filter to possess exact symmetry in its magnitude response, the transfer function must have a denominator with only 1-D (stable) separable factors.

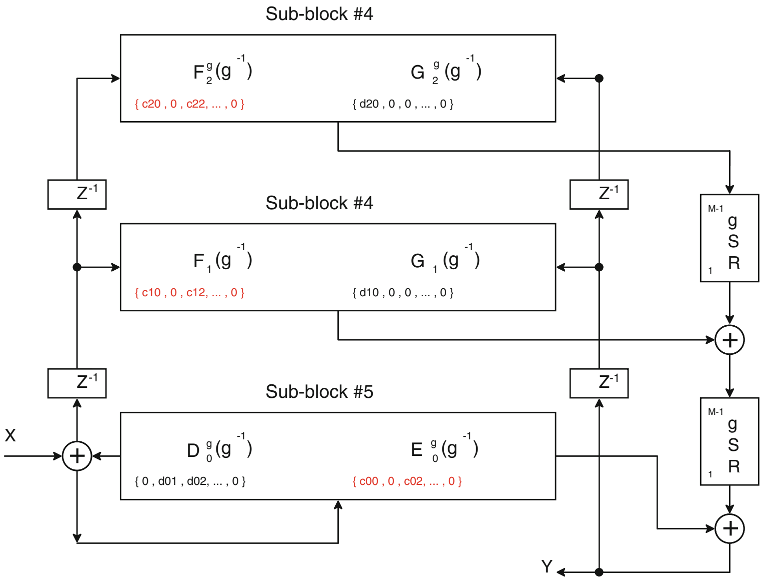

Fig. 27 Delta operator quadrantal symmetry framework based on framework K

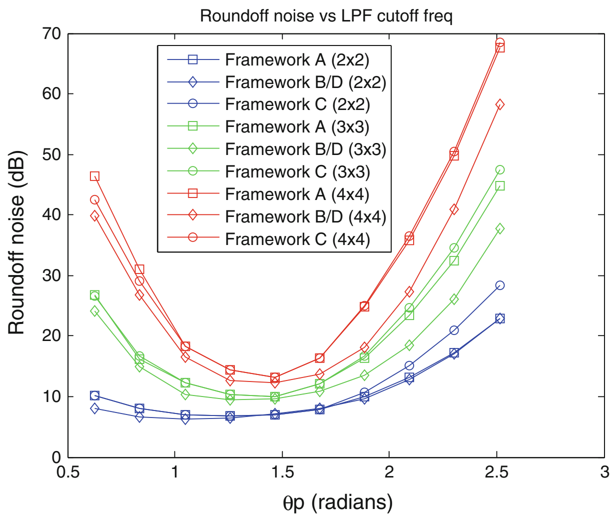

Fig. 28 Roundoff noise

This is needed to ensure that the 2-D filter is BIBO stable while possessing the said symmetry. However, as the denominator is in a constrained form, it may not be possible to meet certain specifications such as sharp cut off in the transition band of the filter magnitude specs. This can force the use of higher order transfer function in the separable case resulting in more expensive implementation. One solution is to utilize a filter design procedure with 2-D non separable denominator factors in the filter transfer function to achieve

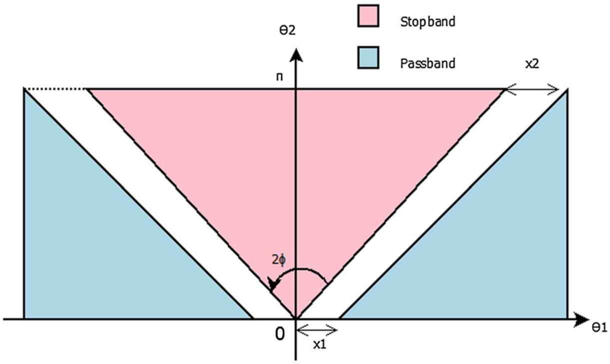

Fig. 29 Fan filter specification

Table 1 4×4 z-domain fan filter results

Filter order	Filter stopband angle (ϕ)(°)	Non-separable design error	Separable design error
4×4	15	23.69	32.27
4×4	25	16.15	27.75
4×4	35	9.77	32.16
4×4	45	14.72	28.63

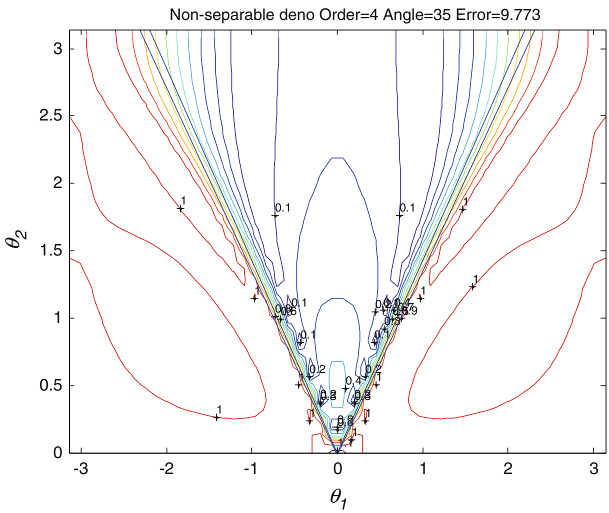

Fig. 30 4×4 non-separable denominator z-domain filter (stopband angle = 35°)

an approximate quadrantal symmetric magnitude response (Lin et al. 1988). In the approach presented in this paper, the numerator of the filter transfer function is still chosen as a quadrantal symmetric polynomial allowing us to reduce the number of multipliers in the final realization as well as to attain the near quadrantal symmetric overall response. The stability problem in the non-separable case is solved by using the planar least squares inverse (PLSI)

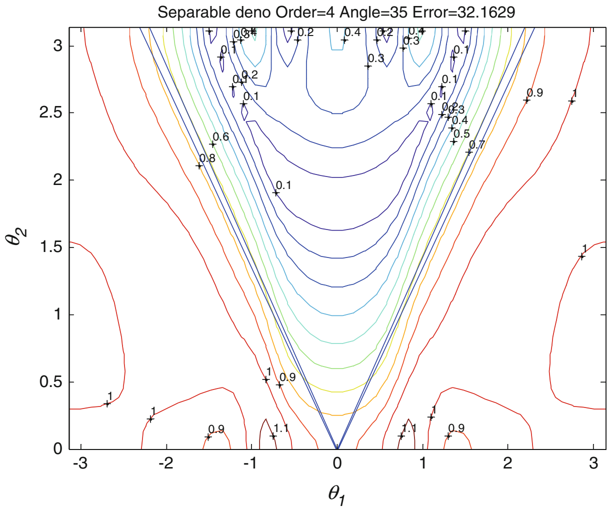

Fig. 31 4×4 separable denominator z-domain filter (stopband angle = 35°)

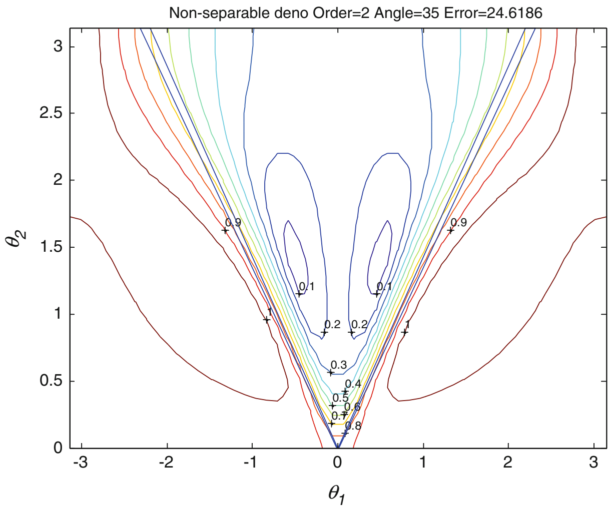

Fig. 32 2×2 non-separable denominator z-domain filter (stopband angle = 35°)

polynomial stabilization approach first established by Anderson and Jury (1976), Jury et al. (1977).

A fan filter with a narrow transition band is used for illustration. The filter magnitude specification is shown in Fig. 29. The filter stopband has an angle of 2ϕ. The filter transition band is specified by x1 = 0.0157 and x2 = 0.113.

Optimization is used to obtain the transfer function that satisfies the fan filter specifications. The objective is to minimize the least squared error between the filter magnitude response and the give filter specifications. The objective or error function is given in (30). It is based

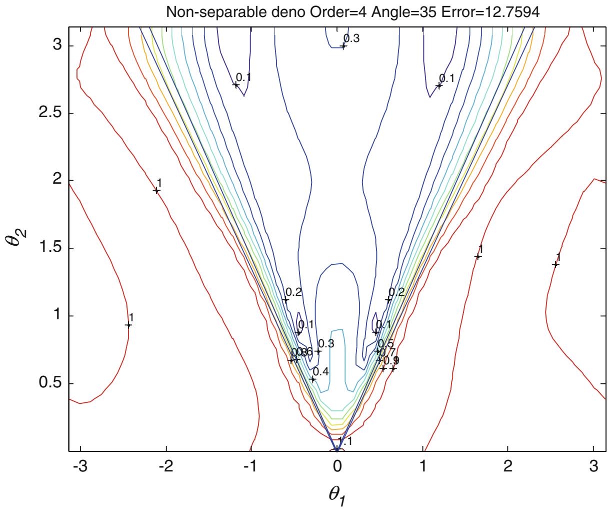

Fig. 33 4×4 non-separable denominator γ-domain filter (stopband angle = 35°)

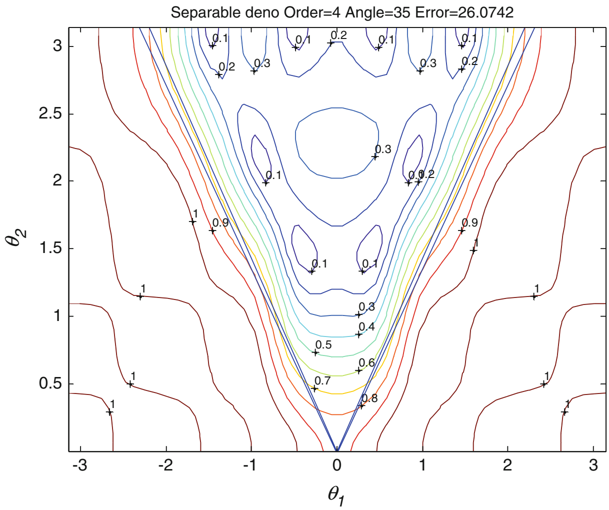

Fig. 34 4×4 separable denominator γ-domain filter (stopband angle = 35°)

Table 2 4×4 γ-domain fan filter results

Filter order	Filter stopband angle (ϕ)(°)	Non-separable design error	Separable design error
4×4	15	20.12	28.10
4×4	25	14.89	23.70
4×4	35	12.76	26.07
4×4	45	11.69	30.13

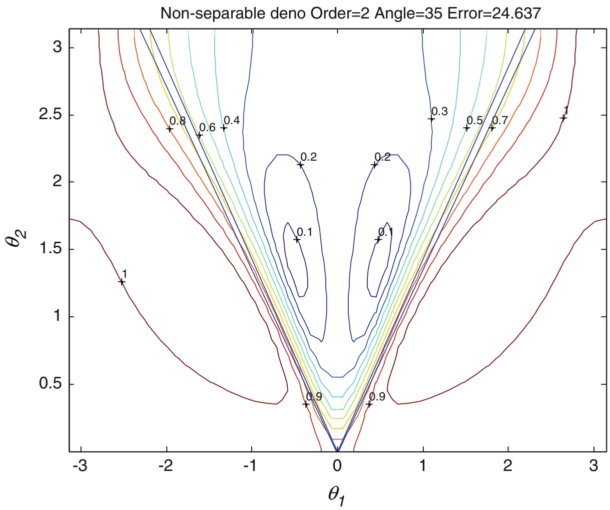

Fig. 35 2×2 non-separable denominator γ-domain filter (stopband angle = 35°)

on the difference between the magnitude response of the transfer function and the desired magnitude response, at selected frequency points in both the passband and stopband.

$$Error = \sum_{k} \sum_{l} \left[F\left(\theta_{1k}, \theta_{2l}\right) - F_d\left(\theta_{1k}, \theta_{2l}\right) \right]^2 \tag{30}$$

where F is the transfer function magnitude squared response, F_d is the desired response, and θ_{1k}, θ_{2l} are the sample frequency points where the desired response is specified.

After optimization, the denominator factors are stabilized, if necessary, using the PLSI approach. The results are shown in Table 1 for a z-domain filter of order 4×4 and different stopband angles. It can be seen that the objective function errors are smaller for the non-separable denominator designs compared to the traditional 1-D separable denominator designs.

The magnitude contour plot for the non-separable denominator design with filter stopband angle of 35 degree is shown in Fig. 30. The corresponding contour plot for the separable denominator design in shown in Fig. 31. It can be seen that non-separable denominator design has a much sharper transition band. The plot also displayed very good quadrantal symmetry despite it being not exact.

The same sharp transition bands can be observed for the 15, 25,45 degree stopband designs. In addition, for certain cases, a non-separable design of lower order may achieve the same error as a separable design. For example, a 2×2 non-separable denominator design has a design error of 24.62, which is slightly smaller than a 4×4 separable design (error of 32.16). Its contour plot is shown in Fig. 32.

Similar observations can be seen in the delta-operator based designs for the same fan filter specifications (Table 2). The non-separable designs have smaller objective function errors and sharper transition bands compared to the separable designs. The results are shown in Figs. 33 and 34. The quadrantal symmetry in the plot for the non-separable design, although not exact, is still quite acceptable.

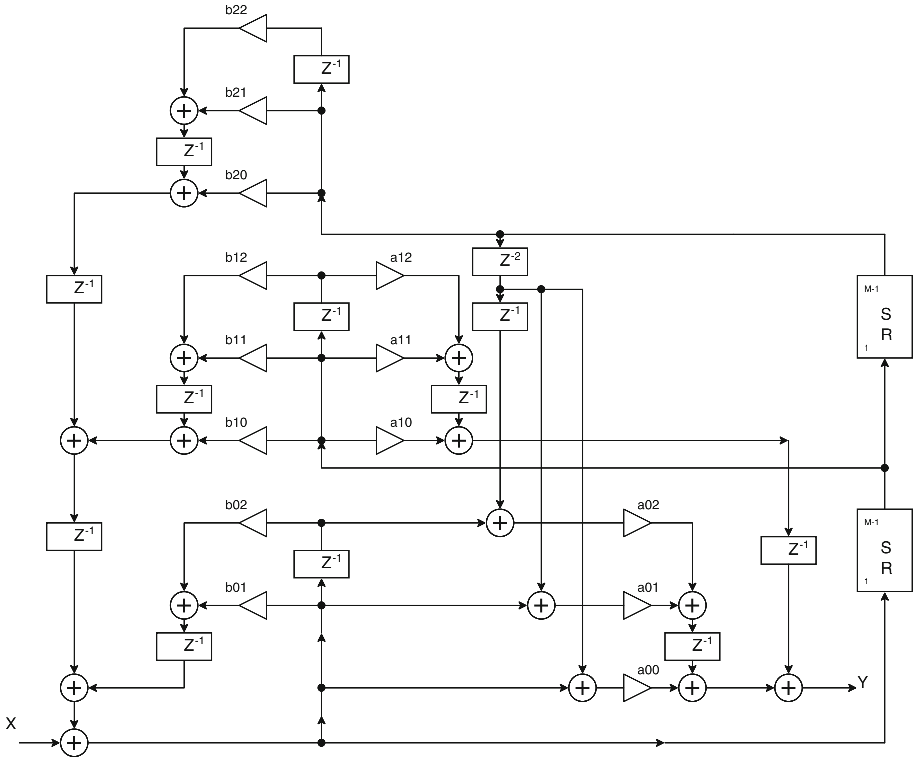

Fig. 36 2×2 filter structure with quadrantal symmetric numerator and non-separable denominator (Type I)

Again, for certain cases, it is possible for a lower order non-separable denominator design to achieve the same performance as a higher order separable design. For example, a 2×2 non-separable denominator γ-domain design has a design error of 24.63, which is slightly smaller than a 4×4 separable design (error of 26.07). It contour plot is shown in Fig. 35.

It can be seen from the example that the non-separable denominator designs with approximate symmetry can achieve a sharper transition band when compared with exact quadrantal symmetric response using a transfer function with separable denominator.

A 2×2 VLSI filter structure realizing a z-domain quadrantal symmetric numerator and non-separable denominator is shown in Fig. 36. An alternate structure based on its transpose is shown in Fig. 37. They can easily be generalized to higher orders.

11 Conclusion

A generalized formulation is presented that allows the derivation of several new 2-D VLSI filter structures using different 1-D filter sub-blocks and different interconnection frameworks. The 1-D sub-blocks are represented by general digital two-pair networks which consist of direct-form or lattice-type FIR filters in one of the frequency variables. Then, by applying the sub-blocks in various frameworks, 2-D structures realizing different transfer functions are easily obtained. The structures cover conventional z-domain filters as well as delta operator

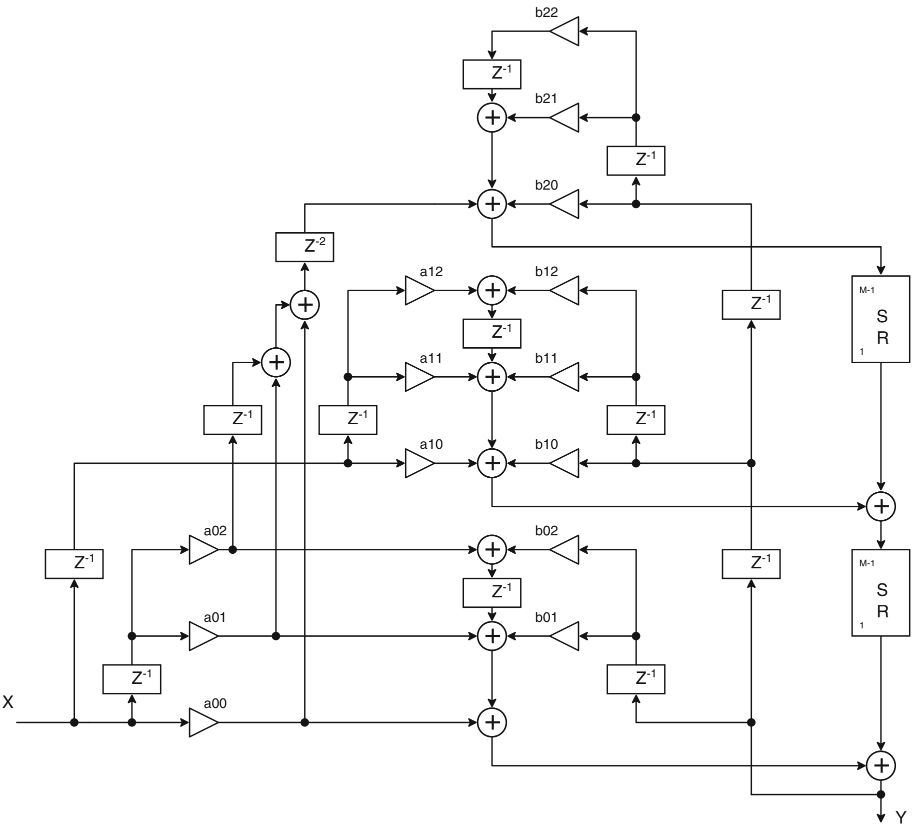

Fig. 37 2×2 filter structure with quadrantal symmetric numerator and non-separable denominator (Type 2).

based filters. These structures can realize general 2-D IIR and FIR transfer functions, IIR transfer functions with separable denominators, and transfer functions with quadrantal magnitude symmetry. The quadrantal symmetry structures have the advantage of lowest number of multipliers.

In Sect. 10, it has been shown that near quadrantal symmetric response could be achieved by choosing (at the optimization stage) a transfer function with a numerator that is a quadrantal symmetric polynomial and a non-separable 2-D denominator polynomial. The advantages of this approach compared to the exact quadrantal symmetric method are also discussed. 2-D VLSI structures without global broadcast are given for the non-separable case.

As a future research problem, the noise and sensitivity properties of the structures, especially for the delta-operator based one, are important topics to investigate. Further, the possibility of extending the structures to cover other types of symmetries (diagonal, four fold rotational and octagonal) needs to be explored. Recently, a new state space formulation was presented for multidimensional signal processing systems (Velten et al. 2012). It is hoped that the block framework structures given in the paper will be useful in the analysis and design with this new state space formulation. It will also be interesting to see whether improved design method could be developed for 2-D filter banks (Zhao and Swmay 2013), based on the present work on structures as well as the optimization steps to achieve approximate symmetry.

Acknowledgments The authors would like to express their sincere thanks to the EIC and his Editorial board members for their kind suggestions to improve the quality of this paper.

References

Agarwal, R. C., & Burrus, C. S. (1975). New recursive digital filter structures having very low sensitivity and roundoff noise. *IEEE Transactions on Circuits and Systems, CAS-22*, 921–927.

Aly, S. A. H., & Fahmy, M. M. (1981). Symmetry exploitation in the design and implementation of two-dimensional rectangularly sampled filters. *IEEE Transactions on Acoustics, Speech and Signal Processing, ASSP-29*, 973–982.

Anderson, B. D. O., & Jury, E. I. (1976). Proof of a special case of Shanks' conjecture. *IEEE Transactions on Acoustics, Speech and Signal Processing*, *24*(6), 574–575.

Bruton, L. T., & Strecker, T. E. (1983). Two-dimensional discrete filters using spatial integrators. *IEE Proceedings, 130*(6), 271–275.

Chen, P. Y., Van, L. D., Khoo, I. H., Reddy, H. C., & Lin, C. T. (2011). Power-efficient and cost-effective 2-D symmetry filter architectures. *IEEE Transactions on Circuits and Systems I: Regular Papers*, *58*(1), 112–125.

Fettweis, A. (1997). Symmetry requirements for multidimensional digital filters. *International Journal of Circuit Theory and Applications*, *5*, 343–353.

George, B. P., & Venetsanopoulos, A. N. (1984). Design of two-dimensional recursive digital filters on the basis of quadrantal and octagonal symmetry. *Circuits, Systems, and Signal Processing*, *3*, 59–78.

Goodwin, G. C., Middleton, R. H., & Poor, H. V. (1992). High-speed digital signal processing and control. *Proceedings of the IEEE*, *80*(2), 240–259.

Joshi, R. M., Madanayake, A., Adikari, J., & Bruton, L. T. (2012). Synthesis and array processor realization of a 2-D IIR beam filter for wireless applications. *IEEE Transactions on Very Large Scale Integration (VLSI) Systems, 20*(12), 2241–2254.

Jury, E. I., Kolavennu, V. R., & Anderson, B. D. O. (1977). Stabilization of certain two-dimensional recursive digital filters. *Proceedings of the IEEE*, *65*(6), 887–892.

Kauraniemi, J., Laakso, T. I., Hartimo, I., & Ovaska, S. J. (1998). Delta operator realizations of direct-form IIR filters. *IEEE Transactions on Circuits and Systems II: Analog and Digital Signal Processing*, *45*(1), 41–52.

Khoo, I. H., Reddy, H. C., & Rajan, P. K. (2006). Symmetry study for delta-operator-based 2-D digital filters. *IEEE Transactions on Circuits and Systems I*, *53*(9), 2036–2047.

Khoo, I. H., Reddy, H. C., Van, L. D., & Lin, C. T. (2009). 2-D digital filter architectures without global broadcast and some symmetry applications. *Proceedings of the 2009 ISCAS* (pp. 952–959).

Khoo, I. H., Reddy, H. C., Van, L. D., & Lin, C. T. (2010). Generalized formulation of 2-D filter structures without global broadcast for VLSI implementation. *Proceedings of the 2010 IEEE international midwest symposium on circuits and systems (MWSCAS)* (pp. 426–429).

Khoo, I. H., Reddy, H. C., Van, L. D., & Lin, C. T. (2012). Delta operator based 2-D VLSI filter structures without global broadcast and incorporation of the quadrantal symmetry. *Proceedings of the 2012 ISCAS* (pp. 3190–3193).

Lin, Z., Bruton, L. T., & Bartley, N. R. (1988). Design of highly selective two dimensional recursive fan filters by relaxing symmetry constraints. *Electronics Letters*, *24*(22), 1361–1362.

Lu, W. S., & Antoniou, A. (1992). *Two-dimensional digital filters*. New York: Dekker.

Makhoul, J. (1978). A class of all-zero lattice digital filters: Properties and applications. *IEEE Transactions on Acoustics, Speech and Signal Processing*, *26*, 304–314.

Middleton, R. H., & Goodwin, G. C. (1986). Improved finite word length characteristics in digital control using delta operators. *IEEE Transactions on Automatic Control*, *31*(11), 1015–1021.

Middleton, R. H., & Goodwin, G. C. (1990). *Digital control and estimation: A unified approach*. Englewood Cliffs: Prentice-Hall.

Premaratne, K., Suarez, J., Ekanayake, M. M., & Bauer, P. H. (1994). Two-dimensional delta-operator formulated discrete-time systems: State-space realization and its coefficient sensitivity properties. *Proceedings of the 37th midwest symposium on circuits and systems* (vol. 2, pp. 805–808).

Rajan, P. K., & Swamy, M. N. S. (1978). Quadrantal symmetry associated with two-dimensional digital filter transfer functions. *IEEE Transactions on Circuits Systems, CAS-25*, 340–343.

Reddy, H. C., Khoo, I. H., & Rajan, P. K. (2003). 2-D symmetry: Theory and filter design applications. *IEEE Circuits and Systems Magazine*, *3*(3), 4–33.

Sid-Ahmed, M. A. (1989). A systolic realization for 2-D digital filters. *IEEE Transactions on Acoustics, Speech and Signal Processing, 37*, 560–565.
Sunder, S., El-Guibaly, F., & Antoniou, A. (1990). Systolic implementations of two-dimensional recursive digital filters. *Proceedings of IEEE international symposium on circuits and systems* (pp. 1034–1037).
Van, L. D. (2002). A new 2-D systolic digital filter architecture without global broadcast. *IEEE Transactions on VLSI Systems*, *10*(4), 477–486.
Velten, J., Schauland, S., & Kummert, A. (2012). Realization of multidimensional signal processing systems given in natural k-D state space description. *Multidimensional Systems and Signal Processing*, *23*(1–2), 281–290.
Wong, N., & Ng, T. S. (2000). Round-off noise minimization in a modified direct-form delta operator IIR structure. *IEEE Transactions on Circuits and Systems II: Analog and Digital Signal Processing*, *47*(12), 1533–1536.
Zhao, Y., & Swmay, M. N. S. (2013). The analysis and design of two-dimensional nearly-orthogonal symmetric wavelet filter banks. *Multidimensional Systems and Signal Processing*, *24*(1), 199–218.

Author Biographies

I-Hung Khoo received his Ph.D. in Electrical and Computer Engineering from the University of California Irvine in 2002. He joined the Department of Electrical Engineering at California State University Long Beach in 2006, where he is currently an Associate Professor. Previously, he was a Senior I. C. Design Engineer at Agilent/Avago Technologies. Dr. Khoo's research interests include high speed circuit design and analog & digital signal processing. He is currently serving as an officer of the IEEE Systems Council Chapter in the Coastal Los Angeles Section.

Hari C. Reddy received his B.E. degree in Electrical Engineering in 1964 from Sri Venkateswara University, Tirupati, India; the M.E. degree in Electrical Engineering from M.S. University of Baroda, Baroda, India in 1966; and the Ph.D. degree in Electronics and Communication Engineering, from Osmania University, Hyderabad, India in 1974. He then did 2 years of post doctoral research work at the Concordia University, Montreal, Canada, 1975–1977. Professor Reddy has been with the Department of Electrical Engineering, California State University, Long Beach (CSULB), as a tenured Full-Professor since 1987. Dr. Reddy was with the Department of Electrical Engineering at Tennessee Technological University, Cookeville, Tennessee as an Associate Professor (1980–1983) and as tenured full professor from 1983–1987. Before joining Tennessee Tech, Dr. Reddy held teaching and research positions at the State University of New York College at Buffalo; Concordia University, Montreal, Canada; Osmania University, Hyderabad India; and S.G.S. Institute of Science and Technology, Indore, India. During the past 10 years he has been a Guest Professor at the Institute for Signal and Information Processing and Institute for Integrated Systems, Swiss Federal Institute of Technology (ETH) Zurich, Switzerland; and Visiting Researcher from 1994 to 1999 in the Department of Electrical and Computer Engineering at the University of California, Irvine, California. In 2003 he has been awarded Honorary Professorship of the Technical University of Iasi, Iasi, Romania. Dr. Reddy's teaching and research interests are in the broad areas of Circuit Design, Filters, Systems and Signal Processing. His research is concerned with the theory and applications of Multidimensional Circuits, Systems and Digital Filters. For the past several years, he has also been working on the development of circuit theory for high speed signal processing and other related problems using delta discrete time operator. He has co-authored about one hundred and twenty five research papers and three book chapters. He attended and presented papers in over fifty international conferences. Dr. Reddy has been interested on the impact of advances of research on Electrical Engineering Education. He was the guest editor for the special issue (Research and Education: Circuits and Systems) of the IEEE Transactions on Education published in August 1989. He served as the Principal Associate Editor for the IEEE Transactions on Education (1984–1990). From 1993 to 1996, he was also an Associate Editor for IEEE Transactions on Circuits and Systems (Part I) and also served as an Associate Editor for the Journal of Circuits, Systems and Computers. In 1999, he co-organized and served as General Chair of the IEEE CAS society's 3rd Emerging Technologies Workshop on Mixed Signal Integrated Circuit Design held in Long Beach, California. Professor Reddy served as the President-elect, President and past President of the IEEE Circuits and Systems Society in 2000, 2001 and 2002 respectively. Earlier, he served as CAS Society's Vice President for the Conferences for 3 years (1996, 1997, 1999). From 1993 to 1995, he was a member of the IEEE CAS Society's Board of Governors. He also served as Chair of the IEEE CAS Society Fellows Committee for 2 years (2003 and 2004). Prof. Reddy is a recipient of the 2003 IEEE Circuits and Systems Society's Meritorious Service Award. Also, in 2003, Prof. Reddy received the diploma of honorary member of the Senate of the Technical University of Iasi, Romania and the "Gh. Asachi" University Medal for outstanding contributions in the activities of cooperation with the faculties of the Technical University. Prof. Reddy was elected as a Fellow of the IEEE in 1992 for contributions in the field of multidimensional circuits and systems. Prof. Reddy is a recipient of the Distinguished Faculty Scholarly and Creative Achievement Award (1990) and the Outstanding Professor Award (1993) from the California State University at Long Beach. He received (at the 1990 & 1992 Commencements) the TRW Excellence in Research and Teaching Awards.

Lan-Da Van received the B.S. (Honors) and the M.S. degree from Tatung Institute of Technology, Taipei, Taiwan, in 1995 and 1997, respectively, and the Ph.D. degree from National Taiwan University (NTU), Taipei, Taiwan, in 2001, all in electrical engineering. From 2001 to 2006, he was an Associate Researcher at National Chip Implementation Center (CIC), Hsinchu, Taiwan. Since Feb. 2006, he joined the faculty of Department of Computer Science, National Chiao Tung University, Hsinchu, Taiwan, where he is currently an Associate Professor. His research interests are in VLSI algorithms, architectures, and chips for digital signal processing (DSP) and biomedical signal processing. This includes the design of low-power/high-performance/low cost 3-D graphics processors, adaptive biomedical systems, computer arithmetic, multidimensional filters, and transforms. He has published more than 45 journal and conference papers in these areas. Dr. Van was a recipient of the Chunghwa Picture Tube (CPT) and Motorola fellowships in 1995 and 1997, respectively. He was an elected chairman of IEEE NTU Student Branch in 2000. In 2001, he has received IEEE award for outstanding leadership and service to the IEEE NTU Student Branch. In 2005, he was a recipient of the Best Poster Award at iNEER Conference for Engineering Education and Research (iCEER). From 2009, he serves as the officer of IEEE Taipei Section. He served as a reviewer for the IEEE TCAS I, the IEEE TCAS II, the IEEE TCSVT, the IEEE TC, the IEEE TCAD, the IEEE TMM, the IEEE TSP, the IEEE TVLSI SYSTEMS, and the IEEE SPL. He is a member of the IEEE.

Chin-Teng Lin received the B.S. degree in control engineering from National Chiao-Tung University (NCTU), Hsinchu, Taiwan, in 1986 and the M.S.E.E. and Ph.D. degrees in electrical engineering from Purdue University, West Lafayette, IN, in 1989 and 1992, respectively. Since August 1992, he has been with the College of Electrical Engineering and Computer Science, NCTU, where he is currently the University Provost and the Chair Professor of Electrical and Control Engineering. He served as the Founding Dean of Computer Science College of NCTU from 2005 to 2007. He is the textbook author of Neural Fuzzy Systems (Prentice-Hall) and Neural Fuzzy Control Systems with Structure and Parameter Learning (World Scientific). He has published over 140 journal papers, including about 80 IEEE Transactions papers. His research interests are in intelligent technology, soft computing, brain–computer interface, smart living technology, intelligent transportation systems, robotics and intelligent sensing, and nanobioinformation technologies and cognitive science (NBIC). Dr. Lin is a member of Tau Beta Pi, Eta Kappa Nu, and Phi Kappa Phi honorary societies. He was a member of the Board of Governors (BoG) of the IEEE Systems, Man, Cybernetics Society (SMCS) from 2003 to 2005 and IEEE Circuit and Systems Society (CASS) (2005–2008), and the current BoG member of IEEE Computational Intelligence Society (CIS) (2008–2010). Dr. Lin is the IEEE Distinguished Lecturer from 2003 to 2005. He served as the Deputy EIC of the IEEE TRANSACTIONS OF CIRCUITS AND SYSTEMS—PART II, EXPRESS BRIEFS (2007–2008). Dr. Lin is the General Chair of FUZZ-IEEE2011 to be held in Taipei, and was the Program Chair of the 2006 IEEE International Conference on Systems, Man, and Cybernetics held in Taipei. He was the president of Board of Government (BoG) of Asia Pacific Neural Networks Assembly (APNNA) from 2004 to 2005. He has won the Outstanding Research Award granted by National Science Council (NSC), Taiwan, from 1997 to the present, the Outstanding Professor Award granted by the Chinese Institute of Engineering (CIE) in 2000, and the 2002 Taiwan Outstanding Information-Technology Expert Award. He was also elected to be one of 38th Ten Outstanding Rising Stars in Taiwan (2000).